Inertial Navigation System Aiding with Orbcomm LEO Satellite Doppler Measurements

Joshua J. Morales, Joe Khalife, Ali A. Abdallah, Christian T. Ardito, and Zaher M. Kassas
University of California, Riverside

BIOGRAPHIES

Joshua J. Morales is a Ph.D. Candidate in the Department of Electrical and Computer Engineering at the University of California, Riverside (UCR) and a member of the Autonomous Systems Perception, Intelligence, and Navigation (ASPIN) Laboratory. He received a B.S. in Electrical Engineering with High Honors from UCR. In 2016 he was accorded an Honorable Mention from the National Science Foundation (NSF). His research interests include estimation theory, navigation systems, autonomous vehicles, and intelligent transportation systems.

Joe J. Khalife is a Ph.D. Candidate at UCR and member of the ASPIN Laboratory. He received a B.E. in Electrical Engineering and an M.S. in Computer Engineering from the Lebanese American University (LAU). From 2012 to 2015, he was a research assistant at LAU. His research interests include opportunistic navigation, autonomous vehicles, and software-defined radio.

Ali A. Abdallah is a Ph.D student at UCR and a member of the ASPIN Laboratory. He received a B.E in Electrical Engineering from the LAU. His current research interests include opportunistic navigation and software-defined radio.

Christian T. Ardito received a B.S. in Electrical Engineering from UCR. He is currently pursuing a Ph.D. at UCR and a member of the ASPIN Laboratory. His research interests include satellite-based navigation, sensor fusion, and software-defined radio.

Zaher (Zak) M. Kassas is an assistant professor at UCR and director of the ASPIN Laboratory. He received a B.E. in Electrical Engineering from LAU, an M.S. in Electrical and Computer Engineering from The Ohio State University, and an M.S.E. in Aerospace Engineering and a Ph.D. in Electrical and Computer Engineering from The University of Texas at Austin. In 2018, he received the NSF Faculty Early Career Development Program (CAREER) Award. His research interests include cyber-physical systems, estimation theory, navigation systems, autonomous vehicles, and intelligent transportation systems.

ABSTRACT

A tightly-coupled inertial navigation system aided by Orbcomm low Earth orbit (LEO) satellite signals is developed. The developed navigation framework enables a navigating vehicle to aid its inertial navigation system (INS) with Doppler measurements drawn from Orbcomm LEO satellite signals in a tightly coupled fashion when global navigation satellite system (GNSS) signals become unusable. Experimental results are presented showing an unmanned aerial vehicle (UAV) aiding its onboard INS with Doppler measurements drawn from two Orbcomm LEO satellites, reducing the final position error from 31.7 m to 8.8 m after 30 seconds of GNSS unavailability.

I. INTRODUCTION

A global navigation satellite system (GNSS)-aided inertial navigation system (INS) makes use of the complementary properties of each individual system: the short-term accuracy and high data rates of an INS and the long-term stability of a GNSS solution to provide periodic corrections. However, in the inevitable event that GNSS signals become unavailable (e.g., in deep urban canyons, near dense foliage, and in the presence of unintentional interference or intentional jamming) or untrustworthy (e.g., during malicious spoofing attacks), the INS's errors will grow unboundedly.

Signals of opportunity (SOPs) have been considered as an alternative navigation source in the absence of GNSS signals [1, 2]. SOPs include AM/FM radio [3, 4], cellular [5, 6], digital television [7, 8], and low Earth orbit (LEO)

Preprint of the 2018 ION GNSS+ Conference Miami, FL, September 24–28, 2018

satellites [9–11]. These signals have been demonstrated to yield a standalone meter-level-accurate navigation solution on ground vehicles [12–15] and a centimeter-level-accurate navigation solution on aerial vehicles [16, 17]. Moreover, these signals have been used as an aiding source for lidar [18, 19] and INS [20, 21].

LEO satellites are particularly attractive aiding sources for a vehicle's INS in GNSS-challenged environments for several reasons: (1) they are around twenty times closer to Earth compared to GNSS satellites which reside in medium Earth orbit (MEO), making their received signals between 300 to 2,400 times more powerful than GNSS signals; (2) thousands of broadband internet satellites will be launched into LEO by OneWeb, SpaceX, Boeing, among others, bringing an abundance of signal sources [22]; and (3) each broadband provider will deploy satellites into unique orbital constellations transmitting at different frequency bands, making their signals diverse in frequency and direction [23].

To exploit LEO satellites for navigation, their positions and clock states, namely the clock bias and drift of the transmitter, must be known. The position of any satellite may be parameterized by its Keplerian elements: eccentricity, semi-major axis, inclination, longitude of the ascending node, argument of periapsis, and true anomaly. These elements are tracked, updated once daily, and made publicly available by the North American Aerospace Defense Command (NORAD) [24]. However, these elements are dynamic and will deviate from their nominally available values due to several sources of perturbing forces, which include non-uniform Earth gravitational field, atmospheric drag, solar radiation pressure, third-body gravitational forces (e.g., gravity of the Moon and Sun), and general relativity [25]. These deviations can cause errors in a propagated satellite orbit as high as three kilometers if not accounted for with corrections. In contrast to GNSS where corrections to the orbital elements and clock errors are periodically transmitted to the receiver in a navigation message, such orbital element and clock corrections may not be available for LEO satellites; in which case they must be estimated along with the receiver's states: orientation, position, velocity, IMU biases, and clock errors.

A framework to estimate the position and clock states of *stationary* terrestrial transmitters while simultaneously aiding a vehicle's INS with pseudorange observables drawn from such transmitters was presented and studied in [20, 26–28]. This paper presents a more complex framework, which enables the tracking of *mobile* LEO transmitters' states. Specifically, a simultaneous tracking and navigation (STAN) framework is presented, which tracks the states of Orbcomm LEO satellites while simultaneously using Doppler measurements extracted from their signals to aid a vehicle's INS. The components of the framework are discussed and its performance is demonstrated through an experiment on an unmanned aerial vehicle (UAV).

The remainder of this paper is organized as follows. Section II describes the LEO satellite signal-aided INS framework and discusses the LEO satellite dynamics model and the receiver measurement model. Section III provides an overview of the Orbcomm satellite system. Section IV presents experimental results demonstrating a UAV navigating with Orbcomm signals using the LEO satellite signal-aided INS framework. Concluding remarks are given in Section V.

II. STAN NAVIGATION FRAMEWORK

An extended Kalman filter (EKF) framework is employed to aid the INS with LEO satellite pseudorange rates and GNSS pseudoranges when available in a tightly-coupled fashion. The proposed framework, illustrated in Fig. 1, works similarly to that of a traditional tightly-coupled GNSS-aided INS with two main differences: (i) the position and clock states of the LEO satellites are unknown to the receiver; hence, they are estimated along with the states of the navigating vehicle and (ii) Doppler measurements are used to aid the INS instead of GNSS pseudoranges. A similar framework was proposed in [20] to aid a vehicle's INS using stationary terrestrial emitters. However, the framework presented in this paper includes a LEO satellite dynamics model since the signals emanate from fast moving LEO satellites instead of stationary terrestrial emitters. The LEO satellites' dynamics model and the receiver's measurement model are discussed next.

A. LEO Satellite Dynamics Model

The satellites' Keplerian elements are contained in publicly available two-line element (TLE) file sets. The information in these files may be used to initialize an orbit propagator, such as a simplified general perturbation (SGP) model to propagate a satellite's orbit [29]. However, the propagated orbit will deviate from its true one due to several sources

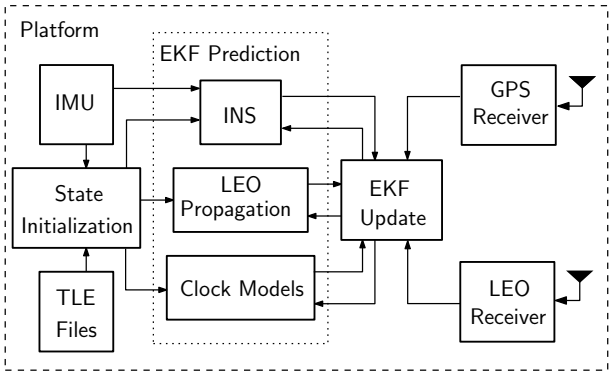

Fig. 1. Tightly-coupled LEO-aided INS navigation framework.

of external force that are not perfectly modeled in SGP models. These deviations can cause large satellite position errors if not accounted for with corrections. In contrast to GNSS where corrections to the orbital elements and clock errors are periodically transmitted to a receiver in a navigation message, such orbital element and clock corrections may not be available for LEO satellites; in which case they must be estimated along with the navigating vehicle's states. There are three common orbital parameterizations used in the orbital determination (OD) literature: (i) position and velocity, (ii) Keplerian elements, and (iii) equinoctial elements. In this work, the position and velocity parameterization was selected since the measurements used to provide corrections are modeled directly as a function of them.

The state vector of the m^{th} LEO satellite will be composed of its three dimensional (3-D) position $\boldsymbol{r}_{\text{leo}_\text{m}}$ and velocity $\dot{\boldsymbol{r}}_{\text{leo}_\text{m}}$ as well as the clock bias and drift of the transceiver equipped on the satellite. The motion equation of the m^{th} LEO satellite is modeled as the sum of the two-body model equation and other perturbing accelerations, give by

$$\ddot{\boldsymbol{r}}_{\text{leo}_\text{m}} = -\frac{\mu}{\|\boldsymbol{r}_{\text{leo}_\text{m}}\|_2^3}\boldsymbol{r}_{\text{leo}_\text{m}} + \tilde{\boldsymbol{a}}_{\text{leo}_\text{m}}, \tag{1}$$

where $\ddot{\boldsymbol{r}}_{\text{leo}_\text{m}} = \frac{d}{dt}\dot{\boldsymbol{r}}_{\text{leo}_\text{m}}$, i.e., the acceleration of the m^{th} LEO satellite, μ is the gravitational constant, and $\tilde{\boldsymbol{a}}_{\text{leo}_\text{m}}$ captures the overall perturbation in acceleration, which includes perturbations caused by non-uniform Earth gravitational field, atmospheric drag, solar radiation pressure, third-body gravitational forces (e.g., gravity of the Moon and Sun), and general relativity [25]. The perturbation vector $\tilde{\boldsymbol{a}}_{\text{leo}_\text{m}}$ is modeled as a white random vector with power spectral density $\mathbf{Q}_{\tilde{a}_{\text{leo}_\text{m}}}$. The m^{th} LEO satellite's clock states time evolution are modeled as a double integrator driven by process noise [30].

B. LEO Satellite Receiver Doppler Measurement Model

The LEO receiver makes Doppler frequency measurements f_D on the available LEO satellite signals, from which a pseudorange rate measurement $\dot{\rho}$ can be obtained from $\dot{\rho} = -\frac{c}{f_c}f_D$, where c is the speed of light and f_c is the carrier frequency. The pseudorange rate measurement $\dot{\rho}_m$ from the m^{th} LEO satellite is modeled according to

$$\dot{\rho}_m(k) = [\dot{\boldsymbol{r}}_{\text{leo}_m}(k) - \dot{\boldsymbol{r}}_r(k)]^{\mathsf{T}} \frac{[\boldsymbol{r}_r(k) - \boldsymbol{r}_{\text{leo}_m}(k)]}{\|\boldsymbol{r}_r(k) - \boldsymbol{r}_{\text{leo}_m}(k)\|_2} + c \cdot \left[\dot{\delta}t_r(k) - \dot{\delta}t_{\text{leo}_m}(k)\right] + c\dot{\delta}t_{\text{iono}_m}(k) + c\dot{\delta}t_{\text{trop}_m}(k) + v_{\dot{\rho}_m}(k),$$

where $\boldsymbol{r}_r$ and $\dot{\boldsymbol{r}}_r$ are the UAV-mounted LEO receiver's 3-D position and velocity vectors, respectively; $\dot{\delta}t_r$ and $\dot{\delta}t_{\text{leo}_m}$ are the UAV-mounted LEO receiver and the m^{th} LEO satellite transmitter clock drifts, respectively; $\dot{\delta}t_{\text{iono}_m}$ and $\dot{\delta}t_{\text{trop}_m}$ are the drifts of the ionospheric and tropospheric delays, respectively, for the m^{th} LEO satellite; and $v_{\dot{\rho}_m}$ is the measurement noise, which is modeled as a white Gaussian random sequence with variance $\sigma^2_{v_{\dot{\rho},m}}$. Note that the variation in the ionospheric and tropospheric delays during LEO satellite visibility is negligible compared to the errors in the satellite's estimated velocities [31]; hence, $\dot{\delta}t_{\text{iono}_m}$ and $\dot{\delta}t_{\text{trop}_m}$ are ignored in the measurement, yielding the measurement model given by

$$\dot{\rho}_m(k) \approx [\dot{\boldsymbol{r}}_{\text{leo}_m}(k) - \dot{\boldsymbol{r}}_r(k)]^{\mathsf{T}} \frac{[\boldsymbol{r}_r(k) - \boldsymbol{r}_{\text{leo}_m}(k)]}{\|\boldsymbol{r}_r(k) - \boldsymbol{r}_{\text{leo}_m}(k)\|_2} + c \cdot \left[\dot{\delta}t_r(k) - \dot{\delta}t_{\text{leo}_m}(k)\right] + v_{\dot{\rho}_m}(k). \tag{2}$$

The next section discusses the Orbcomm LEO satellite constellation from which pseudorange rate measurements are drawn to aid the INS in the experimental test.

III. ORBCOMM SYSTEM

In this section, an overview of the Orbcomm system is provided and the Orbcomm LEO satellite constellation is discussed along with the Orbcomm signals exploited to aid the INS.

A. Orbcomm System Overview

The Orbcomm system is a wide area two-way communication system that uses a constellation of LEO satellites to provide worldwide geographic coverage for sending and receiving alphanumeric packets [32]. The Orbcomm system consists of three main components: (i) subscriber communicators (users), (ii) ground segment (gateways), and (iii) space segment (constellation of satellites), which are briefly discussed next.

(i) Subscriber Communicators (SCs): There are several types of SCs. Orbcomm's SC for fixed data applications uses low-cost very high frequency (VHF) electronics. The SC for mobile two-way messaging is a hand-held, stand-alone unit.

(ii) Ground Segment: The ground segment consists of gateway control centers (GCCs), gateway Earth Stations (GESs), and the network control center (NCC). The GCC provides switching capabilities to link mobile SCs with terrestrial based customer systems via standard communications modes. GESs link the ground segment with the space segment. GESs mainly track and monitor satellites based on orbital information from the GCC and transmit to and receive from satellites, the GCC, or the NCC. The NCC is responsible for managing the Orbcomm network elements and the gateways through telemetry monitoring, system commanding, and mission system analysis.

(iii) Space Segment: Orbcomm satellites are used to complete the link between the SCs and the switching capability at the NCC or GCC.

B. Orbcomm LEO Satellite Constellation

The Orbcomm constellation, at maximum capacity, has up to 47 satellites in 7 orbital planes A–G, illustrated in Fig. 2. Planes A, B, and C are inclined at 45° to the equator and each contains 8 satellites in a circular orbit at an altitude of approximately 815 km. Plane D, also inclined at 45°, contains 7 satellites in a circular orbit at an altitude of 815 km. Plane E is inclined at 0° and contains 7 satellites in a circular orbit at an altitude of 975 km. Plane F is inclined at 70° and contains 2 satellites in a near-polar circular orbit at an altitude of 740 km. Plane G is inclined at 108° and contains 2 satellites in a near-polar elliptical orbit at an altitude varying between 785 km and 875 km.

C. Orbcomm Downlink Signals

The LEO receiver draws pseudorange rate observables from Orbcomm LEO signals on the downlink channel. Satellite radio frequency (RF) downlinks to SCs and GESs are within the 137–138 MHz very high frequency (VHF) band. Downlink channels include 12 channels for transmitting to SCs and one gateway channel, which is reserved for transmitting to the GESs. Each satellite transmits to SCs on one of the 12 subscriber downlink channels through a frequency-sharing scheme that provides four-fold channel reuse. The Orbcomm satellites have a subscriber transmitter that provides a continuous 4800 bits-per-second (bps) stream of packet data using symmetric differential-quadrature phase shift keying (SD-QPSK). Each Satellite also has multiple subscriber receivers that receive short bursts from the SCs at 2400 bps.

Note that Orbcomm satellites are also equipped with a specially constructed 1-Watt ultra high frequency (UHF) transmitter that is designed to emit a highly stable signal at 400.1 MHz. The transmitter is coupled to a UHF antenna designed to have a peak gain of approximately 2 dB. The UHF signal is used by the Orbcomm system for SC positioning. However, experimental data shows that the UHF beacon is absent. Moreover, even if the UHF beacon was present, one would need to be a paying subscriber to benefit from positioning services. Consequently, only downlink channel VHF signals are exploited to aid the INS.

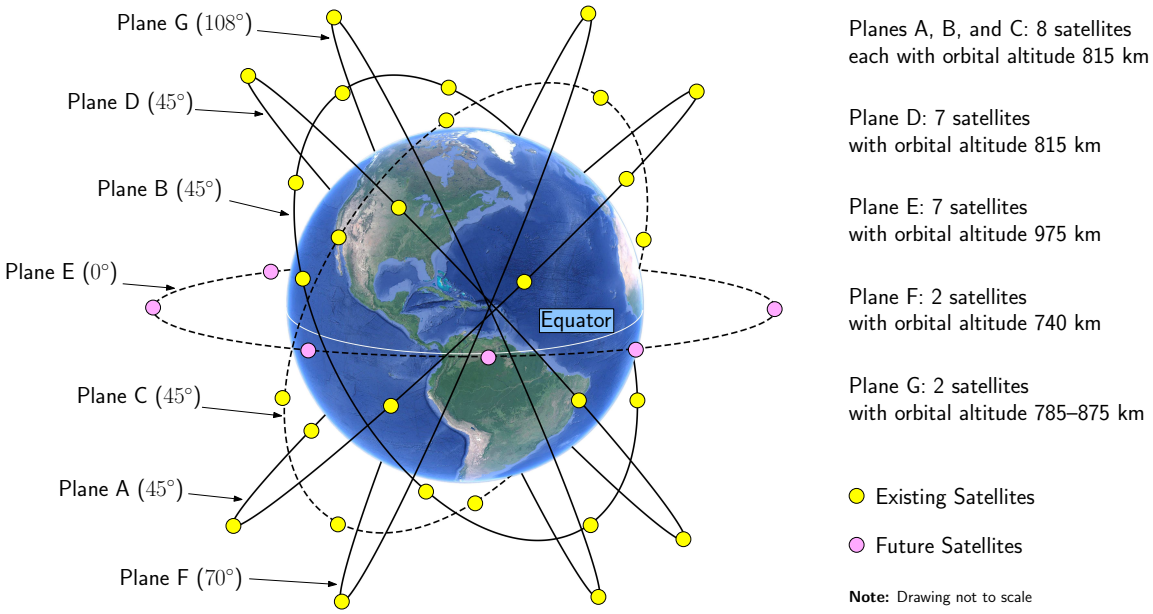

Fig. 2. Orbcomm LEO satellite constellation. Map data: Google Earth.

IV. EXPERIMENTAL RESULTS

In this section, the LEO signal-aided INS framework is demonstrated experimentally on a UAV. The experimental setup is first described and then experimental results are provided.

A. Experimental Setup

An experimental test was conducted to evaluate the performance of the proposed LEO signal-aided INS framework. To this end, a DJI Matrice 600 UAV was equipped with following hardware and software setup:

- A low-cost VHF dipole antenna.
- An RTL-SDR dongle to sample Orbcomm signals.
- A laptop computer to store the sampled Orbcomm signals. These samples were then processed by the Multi-channel Adaptive TRansceiver Information eXtractor (MATRIX) software-defined quadrature phase-shift keying (QPSK) receiver developed by the Autonomous Systems Perception, Intelligence, and Navigation (ASPIN) Laboratory to perform carrier synchronization and extract pseudorange rate observables.
- A Septentrio AsteRx-i V integrated GNSS-IMU, which is equipped with a dual-antenna, multi-frequency GNSS receiver and a Vectornav VN-100 micro-electromechanical system (MEMS) IMU. Septentrio's post-processing software development kit (PP-SDK) was used to process GPS carrier phase observables collected by the AsteRx-i V and by a nearby differential GPS base station to obtain a carrier phase-based navigation solution. This integrated GNSS-IMU real-time kinematic (RTK) system [33] was used to produce the ground truth results with which the proposed navigation framework was compared.

The experimental setup is shown in Fig. 3.

B. Results

The UAV flew a commanded trajectory in Riverside, California over a 120-second period during which 2 Orbcomm LEO satellites were available. Two estimators were implemented to estimate the flown trajectories: (i) the LEO signal-aided INS STAN framework described in Section II and (ii) a traditional GPS-aided INS for comparative analysis.

Each estimator had access to GPS for only the first 90 seconds of the run as illustrated in Fig. 4 (d). Fig. 4

(a) shows the trajectory of the 2 Orbcomm LEO satellites traversed over the course of the experiment. The 3-D position root mean-squared error (RMSE) of the traditional GPS-aided INS's navigation solution after GPS became unavailable was 14.4 meters with a final error of 31.7 meters. The 3-D position RMSE of the UAV's trajectory for the LEO signal-aided INS was 6.8 meters with a final error of 8.8 meters. The estimated satellite trajectory and the along-track, radial, cross-track 99$^{\text{th}}$-percentile final uncertainty ellipse of one of the satellite's position states are illustrated in Fig. 4 (b).

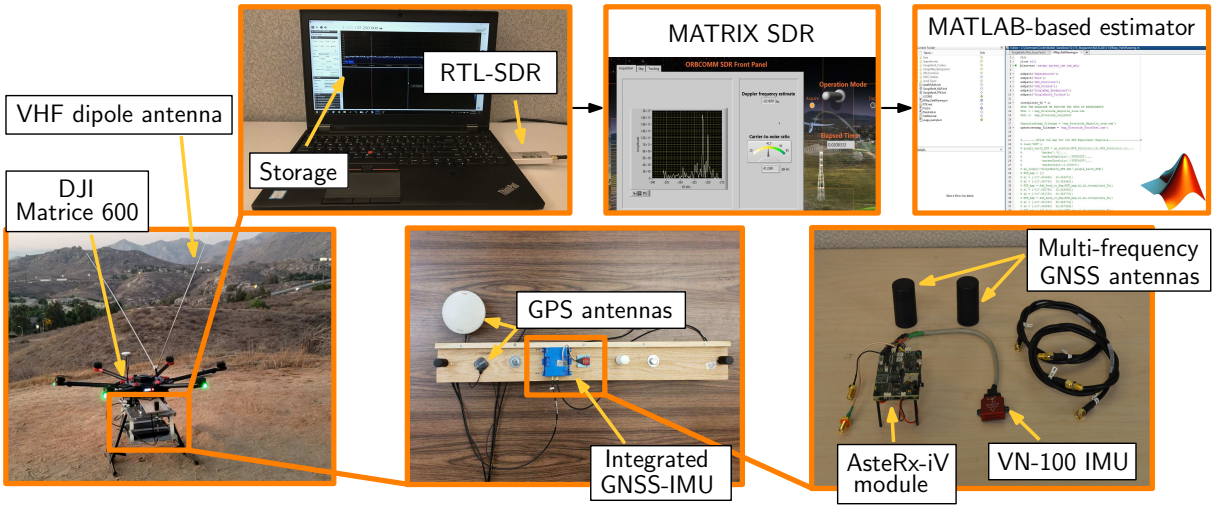

Fig. 3. Experimental setup.

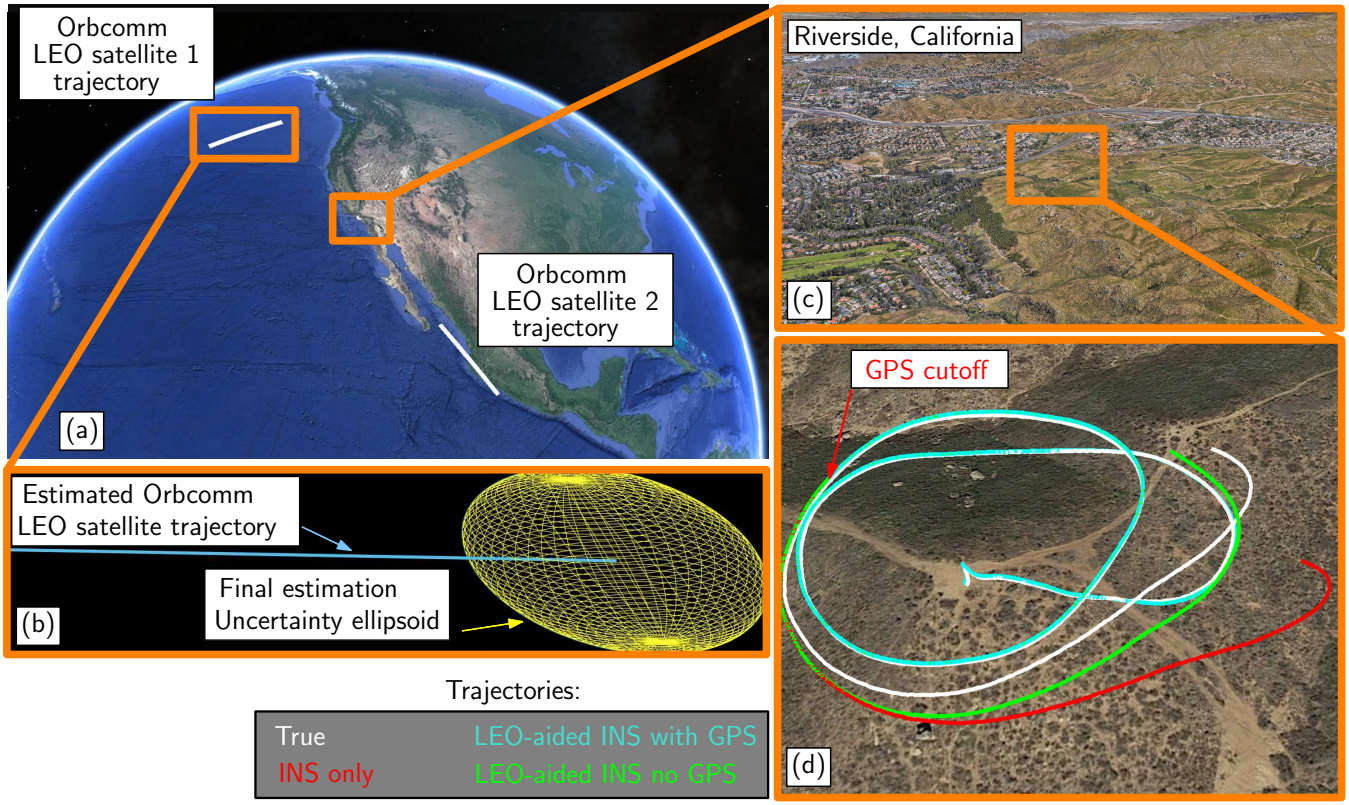

Fig. 4. Experimental results showing (a) the trajectory of the 2 Orbcomm LEO satellites, (b) estimated trajectory of one of the satellites and the final position uncertainty, and (c)–(d) true and estimated trajectories of the UAV.

V. CONCLUSIONS

This work presented a LEO satellite signal-aided INS STAN framework for aiding an INS in the absence of GNSS signals. An overview of the framework and the LEO Orbcomm satellite system was provided. Moreover, experimental results were presented demonstrating a UAV navigating using 2 Orbcomm satellite Doppler measurements in the absence of GNSS. It was demonstrated that the developed framework reduced the UAV's final position error by 72.2% compared to an unaided INS after 30 seconds of GNSS unavailability.

Acknowledgment

This work was supported in part by the Office of Naval Research (ONR) under Grant N00014-16-1-2305 and in part by the National Science Foundation (NSF) under Grant 1751205.

References

[1] L. Merry, R. Faragher, and S. Schedin, "Comparison of opportunistic signals for localisation," in *Proceedings of IFAC Symposium on Intelligent Autonomous Vehicles*, September 2010, pp. 109–114.
[2] Z. Kassas, "Collaborative opportunistic navigation," *IEEE Aerospace and Electronic Systems Magazine*, vol. 28, no. 6, pp. 38–41, 2013.
[3] J. McEllroy, "Navigation using signals of opportunity in the AM transmission band," Master's thesis, Air Force Institute of Technology, Wright-Patterson Air Force Base, Ohio, USA, 2006.
[4] S. Fang, J. Chen, H. Huang, and T. Lin, "Is FM a RF-based positioning solution in a metropolitan-scale environment? A probabilistic approach with radio measurements analysis," *IEEE Transactions on Broadcasting*, vol. 55, no. 3, pp. 577–588, September 2009.
[5] Z. Kassas, J. Khalife, K. Shamaei, and J. Morales, "I hear, therefore I know where I am: Compensating for GNSS limitations with cellular signals," *IEEE Signal Processing Magazine*, pp. 111–124, September 2017.
[6] K. Shamaei, J. Khalife, and Z. Kassas, "Exploiting LTE signals for navigation: Theory to implementation," *IEEE Transactions on Wireless Communications*, vol. 17, no. 4, pp. 2173–2189, April 2018.
[7] M. Rabinowitz and J. Spilker, Jr., "A new positioning system using television synchronization signals," *IEEE Transactions on Broadcasting*, vol. 51, no. 1, pp. 51–61, March 2005.
[8] P. Thevenon, S. Damien, O. Julien, C. Macabiau, M. Bousquet, L. Ries, and S. Corazza, "Positioning using mobile TV based on the DVB-SH standard," *NAVIGATION, Journal of the Institute of Navigation*, vol. 58, no. 2, pp. 71–90, 2011.
[9] M. Joerger, L. Gratton, B. Pervan, and C. Cohen, "Analysis of Iridium-augmented GPS for floating carrier phase positioning," *NAVIGATION, Journal of the Institute of Navigation*, vol. 57, no. 2, pp. 137–160, 2010.
[10] K. Pesyna, Z. Kassas, and T. Humphreys, "Constructing a continuous phase time history from TDMA signals for opportunistic navigation," in *Proceedings of IEEE/ION Position Location and Navigation Symposium*, April 2012, pp. 1209–1220.
[11] T. Reid, A. Neish, T. Walter, and P. Enge, "Leveraging commercial broadband LEO constellations for navigating," in *Proceedings of ION GNSS Conference*, September 2016, pp. 2300–2314.
[12] C. Yang, T. Nguyen, and E. Blasch, "Mobile positioning via fusion of mixed signals of opportunity," *IEEE Aerospace and Electronic Systems Magazine*, vol. 29, no. 4, pp. 34–46, April 2014.
[13] J. Khalife and Z. Kassas, "Navigation with cellular CDMA signals – part II: Performance analysis and experimental results," *IEEE Transactions on Signal Processing*, vol. 66, no. 8, pp. 2204–2218, April 2018.
[14] M. Driusso, C. Marshall, M. Sabathy, F. Knutti, H. Mathis, and F. Babich, "Vehicular position tracking using LTE signals," *IEEE Transactions on Vehicular Technology*, vol. 66, no. 4, pp. 3376–3391, April 2017.
[15] K. Shamaei and Z. Kassas, "LTE receiver design and multipath analysis for navigation in urban environments," *NAVIGATION, Journal of the Institute of Navigation*, 2018, accepted.
[16] J. Khalife and Z. Kassas, "Precise UAV navigation with cellular carrier phase measurements," in *Proceedings of IEEE/ION Position, Location, and Navigation Symposium*, April 2018, pp. 978–989.
[17] J. Khalife, K. Shamaei, S. Bhattacharya, and Z. Kassas, "Centimeter-accurate UAV navigation with cellular signals," in *Proceedings of ION GNSS Conference*, September 2018, accepted.
[18] J. Khalife, S. Ragothaman, and Z. Kassas, "Pose estimation with lidar odometry and cellular pseudoranges," in *Proceedings of IEEE Intelligent Vehicles Symposium*, June 2017, pp. 1722–1727.
[19] M. Maaref, J. Khalife, and Z. Kassas, "Lane-level localization and mapping in GNSS-challenged environments by fusing lidar data and cellular pseudoranges," *IEEE Transactions on Intelligent Vehicles*, 2018, accepted.
[20] J. Morales, P. Roysdon, and Z. Kassas, "Signals of opportunity aided inertial navigation," in *Proceedings of ION GNSS Conference*, September 2016, pp. 1492–1501.
[21] Z. Kassas, J. Morales, K. Shamaei, and J. Khalife, "LTE steers UAV," *GPS World Magazine*, vol. 28, no. 4, pp. 18–25, April 2017.
[22] T. Reid, A. Neish, T. Walter, and P. Enge, "Broadband LEO constellations for navigation," *NAVIGATION, Journal of the Institute of Navigation*, vol. 65, no. 2, pp. 205–220, 2018.
[23] D. Lawrence, H. Cobb, G. Gutt, M. OConnor, T. Reid, T. Walter, and D. Whelan, "Navigation from LEO: Current capability and future promise," *GPS World Magazine*, vol. 28, no. 7, pp. 42–48, July 2017.
[24] North American Aerospace Defense Command (NORAD), "Two-line element sets," http://celestrak.com/NORAD/elements/.
[25] J. Vetter, "Fifty years of orbit determination: Development of modern astrodynamics methods," *Johns Hopkins APL Technical Digest*, vol. 27, no. 3, pp. 239–252, November 2007.
[26] J. Morales, J. Khalife, and Z. Kassas, "Collaborative autonomous vehicles with signals of opportunity aided inertial navigation systems," in *Proceedings of ION International Technical Meeting Conference*, January 2017, 805–818.
[27] J. Morales and Z. Kassas, "Distributed signals of opportunity aided inertial navigation with intermittent communication," in *Proceedings of ION GNSS Conference*, September 2017, pp. 2519–2530.
[28] J. Morales and Z. Kassas, "A low communication rate distributed inertial navigation architecture with cellular signal aiding," in *Proceedings of IEEE Vehicular Technology Conference*, 2018, pp. 1–6.

[29] D. Vallado and P. Crawford, "SGP4 orbit determination," in *Proceedings of AIAA/AAS Astrodynamics Specialist Conference and Exhibit*, August 2008.
[30] Z. Kassas and T. Humphreys, "Observability analysis of collaborative opportunistic navigation with pseudorange measurements," *IEEE Transactions on Intelligent Transportation Systems*, vol. 15, no. 1, pp. 260–273, February 2014.
[31] P. Misra and P. Enge, *Global Positioning System: Signals, Measurements, and Performance*, 2nd ed. Ganga-Jamuna Press, 2010.
[32] Orbcomm, "Networks: Satellite," https://www.orbcomm.com/en/networks/satellite, accessed September 30, 2018.
[33] (2018) Septentrio AsteRx-i V. [Online]. Available: https://www.septentrio.com/products